Quaternary Science Reviews 45 (2012) 85–94

Contents lists available at SciVerse ScienceDirect

Quaternary Science Reviews

journal homepage: www.elsevier.com/locate/quascirev

Testing the robustness of a precipitation proxy-based North Atlantic Oscillation reconstruction

Flavio Lehner [a,b,*], Christoph C. Raible [a,b], Thomas F. Stocker [a,b]

[a] Climate and Environmental Physics, Physics Institute, University of Bern, Switzerland
[b] Oeschger Centre for Climate Change Research, University of Bern, Switzerland

ARTICLE INFO

Article history:
Received 16 December 2011
Received in revised form
24 April 2012
Accepted 30 April 2012
Available online xxx

Keywords:
North Atlantic Oscillation
Climate reconstruction
Proxy validation
Climate model simulations
Last millennium

ABSTRACT

The reconstruction of past atmospheric circulation is crucial for the understanding of natural climate change and its driving factors. A recent reconstruction suggests that, during Medieval times, the European region was dominated by a persistent positive phase of the North Atlantic Oscillation (NAO), followed by a shift to a more oscillatory behavior. We test this hypothesis and the concept underlying the reconstruction in a pseudo-proxy approach using instrumental records, reanalysis data sets and millennial simulations with four different climate models. While a shift from a more positive to a more negative phase of the NAO seems to be likely, the amplitude and persistence of the reconstructed positive phase cannot be reproduced by models. The analysis further reveals that proxy locations that were used in the reconstruction are not always sufficient to describe the NAO. This is reflected in a failure of the reconstruction to verify against instrumental records of the NAO in the 19th century. By adding complementary proxies, the robustness of an NAO reconstruction can be improved to the degree that it would withstand the tests presented here.

1. Introduction

The North Atlantic Oscillation (NAO) is the dominant mode of atmospheric winter circulation over the North Atlantic and European region and is characterized by a meridional gradient in the distribution of atmospheric mass over the North Atlantic (Hurrell, 1995; Wanner et al., 2001). The NAO modulates the extra-tropical zonal flow and its positive and negative phases exhibit a strong control on northern and southern European seasonal temperature and precipitation. Therefore, the NAO has been of interest to human society and science for more than a century. Usually, the NAO is described by an index of the difference in normalized sea level pressure (SLP) over Iceland and the Azores (Rogers, 1984) whereby a high index corresponds to a deepened Icelandic Low and a strengthened Azores High. There are a number of robust alternatives to this classical definition of the NAO index. To mention the most commonly used ones: the principal component (PC) of the leading Empirical Orthogonal Function of the winter SLP in the North Atlantic-European sector (hereafter PC-based; e.g., Kutzbach, 1970), the normalized SLP difference between Iceland and Lisbon (e.g., Hurrell, 1995), or between Iceland and Gibraltar (e.g., Jones et al., 1997). The latter index represents the longest instrumental time series of the NAO, going back to 1821 AD (Vinther et al., 2003).

However, in order to learn about the low-frequency variability and stability of the atmospheric patterns associated with the NAO, longer time series of the index are needed (Wanner et al., 2001, and references therein). Such an extension beyond the instrumental period can be achieved by using proxy data to reconstruct the NAO index over the past centuries (e.g., Appenzeller et al., 1998; Cook et al., 1998, 2002; Luterbacher et al., 1999, 2002; Cullen et al., 2001; Glueck and Stockton, 2001; Rodrigo et al., 2001; Mann, 2002; Casty et al., 2007; Trouet et al., 2009; Kuettel et al., 2010).

In the last years, several reconstruction attempts resulted in a diverse picture of the evolution of the NAO over past centuries (for an overview see, e.g., Pinto and Raible, 2012). The longest reconstruction (Trouet et al., 2009) reported an intriguingly persistent positive NAO index during the Medieval Climate Anomaly (MCA), which shifts into a more oscillatory behavior during the subsequent Little Ice Age (LIA). The MCA refers to the period ~1000–1250 AD, during which relatively high solar irradiance prevailed together with a pause in large eruptions of tropical volcanoes (Fig. 1), causing widespread warming on the Northern Hemisphere. The LIA (~1450–1700 AD) then featured decreased solar activity and an elevated volcanic activity, leading to a cooling. For a recent discussion on the timing and spatial characteristics of the MCA and LIA the reader is referred to Mann et al. (2009).

* Corresponding author. Tel.: +41 316318601.
E-mail address: lehner@climate.unibe.ch (F. Lehner).

0277-3791/$ – see front matter © 2012 Elsevier Ltd. All rights reserved.
doi:10.1016/j.quascirev.2012.04.025

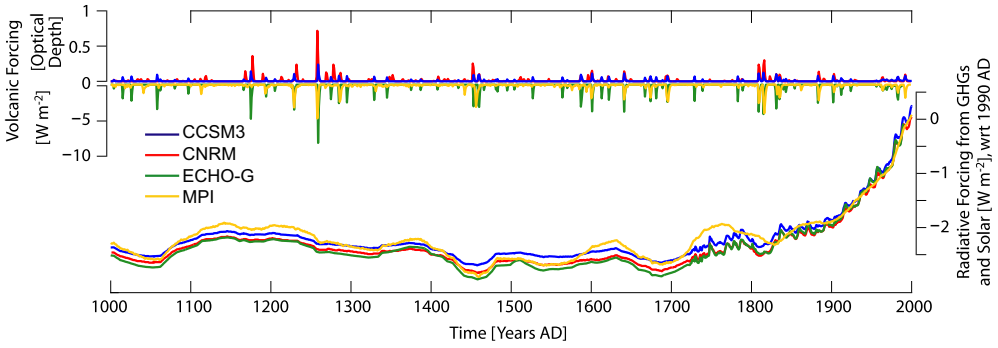

Fig. 1. Forcing used in the different model simulations, given as cumulative radiative forcing from greenhouse gases (GHGs: CO_2, N_2O, CH_4, calculated as in IPCC (2001)) and solar irradiance (right *y*-axis), with reference to (wrt) 1990 AD. For MPI, an Earth System Model that interactively calculates the CO_2, the mean CO_2 of the three ensemble members is used. Forcing from volcanic eruptions is given as optical depth (CCSM3, CNRM) and W m^{-2} (ECHO-G, MPI) (left *y*-axis).

The shift of the NAO suggested by Trouet et al. (2009) implies a fundamental change in dynamics and, if true, should be understood from a mechanistic point of view. Arising from tropical sea surface temperature anomalies, this NAO shift was proposed as a dynamical explanation for the European temperature evolution during that time. However, contradictory evidence from other proxy data suggests changes in winter-spring storminess to have been the distinct feature of the MCA-LIA climate transition in the North Atlantic-European area around 1400 AD (Meeker and Mayewski, 2002). Increased storminess, however, is usually expected to go along with more positive NAO values. A recent reconciliation of proxies and models provides a first explanation on how the two seemingly contradictory signals could be merged into a coherent story (Trouet et al., 2012). Robust reconstructions of past circulation changes are in any case a prerequisite to further improve our understanding of naturally forced climate change such as the MCA-LIA transition.

In the reconstruction of the NAO index, Trouet et al. (2009) used a precipitation proxy from Scotland (width of luminescent bands in a stalagmite from a sub-moorland cave) and a drought proxy from Morocco (combination of 326 time series of ring width from cedars in the Atlas mountains) to describe the two hydrological centers of action that typically arise from an anomalous NAO: a rain band across the northern North Atlantic with increased precipitation in Scotland and western Scandinavia together with drier conditions in the western Mediterranean region in the case of a positive NAO index; and vice versa for the negative case (e.g., Hurrell, 1995; Wanner et al., 2001). The NAO reconstruction by Trouet et al. (2009) can be validated against the instrumental time series of the NAO in the time of overlap. When going beyond that, however, one has to assume a stable relationship between the proxy signal and the NAO index without being able to validate this assumption. By default, proxies are stationary in space and time, while atmospheric patterns are not (Raible et al., 2006). This challenges the stationarity assumption inherent in proxy-based reconstructions and calls for additional validation procedures applicable to these reconstructions.

The aim of this paper is to use reanalysis data and results from simulations with comprehensive climate models to test the longest proxy-based reconstruction of the NAO with respect to (1) the potential occurrence of persistent positive or negative phases of the NAO, (2) the robustness of certain proxy locations in describing centers of action of the NAO, and (3) the possibility of improving the reconstruction by additional proxies. Regarding the third point, our goal is to achieve an improvement of the reconstruction in a minimalistic approach, i.e., by providing only one additional proxy in the proximity of each NAO-related hydrological center of action.

In Section 2 we give a brief overview of the models and reanalysis data sets used as well as the methodology applied. The results are presented in Section 3, subdivided in results from instrumental data, reanalyses and models. A discussion and conclusions follow in Sections 4 and 5.

2. Data and methods

For our analysis we use output from four coupled general circulation models of comparable complexity as well as two state-of-the-art reanalysis data sets (Table 1). The models CNRM-CM3.3 (Salas-Mélia et al., 2005; Swingedouw et al., 2011, hereafter CNRM), ECHO-G (González-Rouco et al., 2006), MPI-ESM (Jungclaus et al., 2010, hereafter MPI), and CCSM3 (low-resolution version, Hofer et al., 2011) were all run for the past millennium, an ensemble of four simulations with CCSM3 was run from 1500 to 2000 AD (used in, e.g., Lehner et al., in press). In addition, an ensemble of six simulations over the time period 1149–1499 AD was carried out with the medium-resolution CCSM3. This last time period corresponds to the transition phase from the MCA to the LIA.

The forcings from greenhouse gases (GHGs), total solar irradiance (TSI) and volcanic eruptions that were applied in the different simulations are shown in Fig. 1. While there exists some consensus on past variations of GHGs, the amplitude of the TSI is still a topic of debate (e.g., Steinhilber et al., 2009; Gray et al., 2010; Shapiro et al., 2011). The TSI reconstructions used here are all in the same range of having a relatively large amplitude (approximately −3.5 W m^{-2} during the Maunder Minimum compared to 1950–2000 AD). All models exhibit a realistic Northern Hemisphere temperature evolution over the past millennium representing a warm MCA and a cold LIA (for further details see references in Table 1). This temperature decrease from the MCA to the LIA is also recorded in proxies of the Central European

Table 1
Model simulations and reanalysis data used in this study. Note that Mitchell and Jones (2005) refers to CRU TS 2.1, while we use the newer version CRU TS 3.0 for which a publication is in preparation.

Model or data set	Resolution (atm/atm levels/ocn)	Time period used (number of runs)	Reference
CCSM3	T31/26/~3° × 3°	1000–2000 AD (1)	Hofer et al. (2011)
CCSM3	T31/26/~3° × 3°	1500–2000 AD (4)	Lehner et al. (in press)
CCSM3	T42/26/~1° × 1°	1149–1499 AD (6)	This study
CNRM	T63/31/~2° × 0.5–2°	1000–1999 AD (1)	Swingedouw et al. (2011)
ECHO-G	T30/19/~2.8° × 2.8°	1000–1990 AD (2)	González-Rouco et al. (2006)
MPI	T31/19/~3° × 3°	1000–2000 AD (3)	Jungclaus et al. (2010)
CRU Reanalysis	1° × 1°	1901–2009 AD (1)	Mitchell and Jones (2005)
20CR	2° × 2°	1871–2008 AD (56)	Compo et al. (2011)

region (e.g., Mangini et al., 2005). Mangini et al. (2005) is an Alpine winter temperature proxy used by Trouet et al. (2009) to illustrate the potential influence of the NAO on European winter temperature. The models simulate a cooling at this location as well (not shown), despite not simulating an MCA-LIA NAO decrease of the magnitude suggested by Trouet et al. (2009).

Regarding atmospheric modes, the models are able to reproduce the temporal and spatial patterns of the NAO with intermediate skill (CNRM, ECHO-G, MPI) and with good skill (CCSM3) (Stoner et al., 2009). As a reference Stoner et al. (2009) used the ERA-40 and NCEP reanalysis data sets which cover only the second half of the 20th century. Bearing in mind the 30-years resolution of the proxy NAO reconstruction, the ERA-40 and NCEP data sets are not of adequate length to be used in this study. We therefore refer to two slightly longer reanalyses (which, nevertheless, are relatively short): the station data-constrained precipitation and temperature reanalysis from the Climate Research Unit (CRU; Mitchell and Jones, 2005) and the hindcast ensemble simulation from the Twentieth Century Reanalysis Project (20CR; Compo et al., 2011). Additionally, we use several instrumental NAO indices going further back in time to test our results. It has been shown by Schmutz et al. (2000) and Cook et al. (2002, after Schmutz et al. (2000)) that the length of the validation/calibration period is crucial for the outcome of a reconstruction and that therefore the longest available instrumental time series should be used.

The model output and the reanalysis data sets are used in a perfect pseudo-proxy approach (e.g., Zorita et al., 2003) to mimic the two proxies used by Trouet et al. (2009) for a reconstruction of the NAO index over the past millennium. The qualifier "perfect" refers to the fact that we do not add artificial noise to the pseudo-proxy but assume the model simulation to represent reality. To mimic the first proxy, the Scotland stalagmite from Proctor et al. (2000), December–March precipitation from northern Scotland is extracted from models and reanalysis (hereafter P_s). For the second proxy, the tree ring-based drought reconstruction by Esper et al. (2007), the Standardized Precipitation Index (SPI; e.g., Guttman, 1999) is calculated from precipitation over Morocco and then averaged from February–June (P_m). These two pseudo-proxies are then treated as in Trouet et al. (2009) to calculate an NAO index: smoothed with a 30-year cubic spline, normalized over a common period, and subtracted from each other. As in Trouet et al. (2009), this index is hereafter called NAO_{ms}. To investigate the sensitivity of the NAO_{ms} to the geographical location of the precipitation signal in models and reanalyses, we vary the averaging box for both proxy sites (four boxes each for Scotland and Morocco; see Fig. 2a). Additionally, we use December–March sea level pressure values from model simulations and 20CR to calculate PC-based (over domain 25–80°N/70°W-40°E), Iceland-Azores, Iceland-Lisbon, and Iceland-Gibraltar NAO indices, which are the commonly accepted, or classical, NAO indices (boxes, over which sea level pressure is averaged are marked in Fig. 2a). The corresponding station data-based indices are provided by the Climate Analysis Section of the National Center for Atmospheric Research in Boulder (Hurrell (1995); www.cgd.ucar.edu/cas/jhurrell/indices.html [November 2011]).

3. Results

In a first step, the agreement of NAO_{ms} with classical NAO indices is tested in a surrogate of the real world – station data and reanalysis data sets. Thereby, we extend the set of tests that can be conducted compared to Trouet et al. (2009) both temporally and in terms of available data sets. In a second step, NAO_{ms} is calculated from output of 17 transient simulations with four different models, totaling roughly 11,000 model years. In this approach we are interested more in the concept behind NAO_{ms} and its robustness over time.

3.1. Instrumental data

In Fig. 2 the classical NAO indices (from station data) are plotted together with different realizations of the NAO_{ms} to test their agreement. Fig. 2b shows the actual proxies used by Trouet et al. (2009) and the NAO_{ms} together with the longest instrumental NAO index (1821–present, though the first two winter contain data gaps; Vinther et al., 2003), all as 30-yr smoothed time series. Surprisingly, the correlation over the full common period 1823–1993 AD of the sole Scotland precipitation proxy ($P_{s\ proxy}$) with the instrumental NAO index (1823–1993 AD: $r_{P_{s\ proxy}|NAO_{Vinther}} = 0.90$, $p < 0.01$) is slightly higher than the correlation of NAO_{ms} with the instrumental NAO index (1823–1993 AD: $r_{NAO_{ms}|NAO_{Vinther}} = 0.81$, $p < 0.05$). Restricting the correlation to different segments of the full period reveals that the Morocco proxy supports the NAO_{ms} only during the period of 1914–1993 AD when $r_{NAO_{ms}|NAO_{Vinther}}$ is larger than $r_{P_{s\ proxy}|NAO_{Vinther}}$ ($p < 0.3$), i.e., when the inclusion of the Morocco proxy improves the correlation. Using a longer time period, the NAO_{ms} is less, or at best equally well correlated with the instrumental NAO index than is the sole Scotland precipitation proxy. Thus, the Morocco proxy seems to add little to the stability and accuracy of the NAO_{ms}. During the 19th century (1823–1899 AD), the correlation of both proxies, and consequently the NAO_{ms}, with the instrumental NAO index strongly decreases, suggesting that during that time neither the sole proxies nor the combined index can correctly describe the instrumental NAO index (visible also in Fig. 2b). This raises the question whether the validation period adopted in Trouet et al. (2009) is long enough and whether the proxies are capable of always adequately capturing the signal of the NAO's northern and southern centers of action. Note, that the correlations on the 30-year smoothed 19th century records are not significant due to the reduced number of degrees of freedom. Further, there remains some doubt about the reliability of the early instrumental pressure records due to missing metadata and data inhomogeneities (Vinther et al., 2003).

3.2. Reanalyses

For both reanalysis data sets the classical NAO indices agree well among each other (Fig. 2c,d). The correlation between PC-based, Iceland-Azores, Iceland-Lisbon, and Iceland-Gibraltar on basis of December–March means is 0.69–0.92 ($p < 0.001$; 20CR: 1871–2008 AD; CRU: 1901–2009 AD; Fig. 3a). These different indices are distributed across the estimated range of spatial variability of the NAO centers of action (Fig. 2a, see also Wanner et al., 2001). Therefore, they are potentially able to also capture the non-stationary spatial behavior of the NAO (at least for the winter NAO; Portis et al., 2001) and are regarded as a robust measure of the atmospheric circulation associated with the NAO.

In Fig. 2c the CRU data set is used as a source for the pseudo-proxies, i.e., to calculate NAO_{ms}. The gray shadings each represent 16 realizations (4 × 4 different boxes) of NAO_{ms}. Along with that, station data-based NAO indices are plotted. While reproducing the most recent decadal-scale negative-to-positive anomaly of the NAO, the NAO_{ms} starts to diverge from the classical indices around the middle of the 20th century and further back. Fig. 2c also features the seasonal (December–March), unsmoothed NAO_{ms} calculated from CRU (lightest gray shading). The comparison with the normal NAO_{ms} suggests that through the normalization after the smoothing an apparently persistent strong ($>1.5\sigma$) positive or negative phase of the NAO can be obtained whereas actually there is just an increased frequency of more positive or negative seasons (not necessarily with an average of $\geq 1.5\sigma$). This is important to keep in mind when interpreting either the persistent +2 phase of the Medieval NAO_{ms} by Trouet et al. (2009) or any smoothed index presented in the study

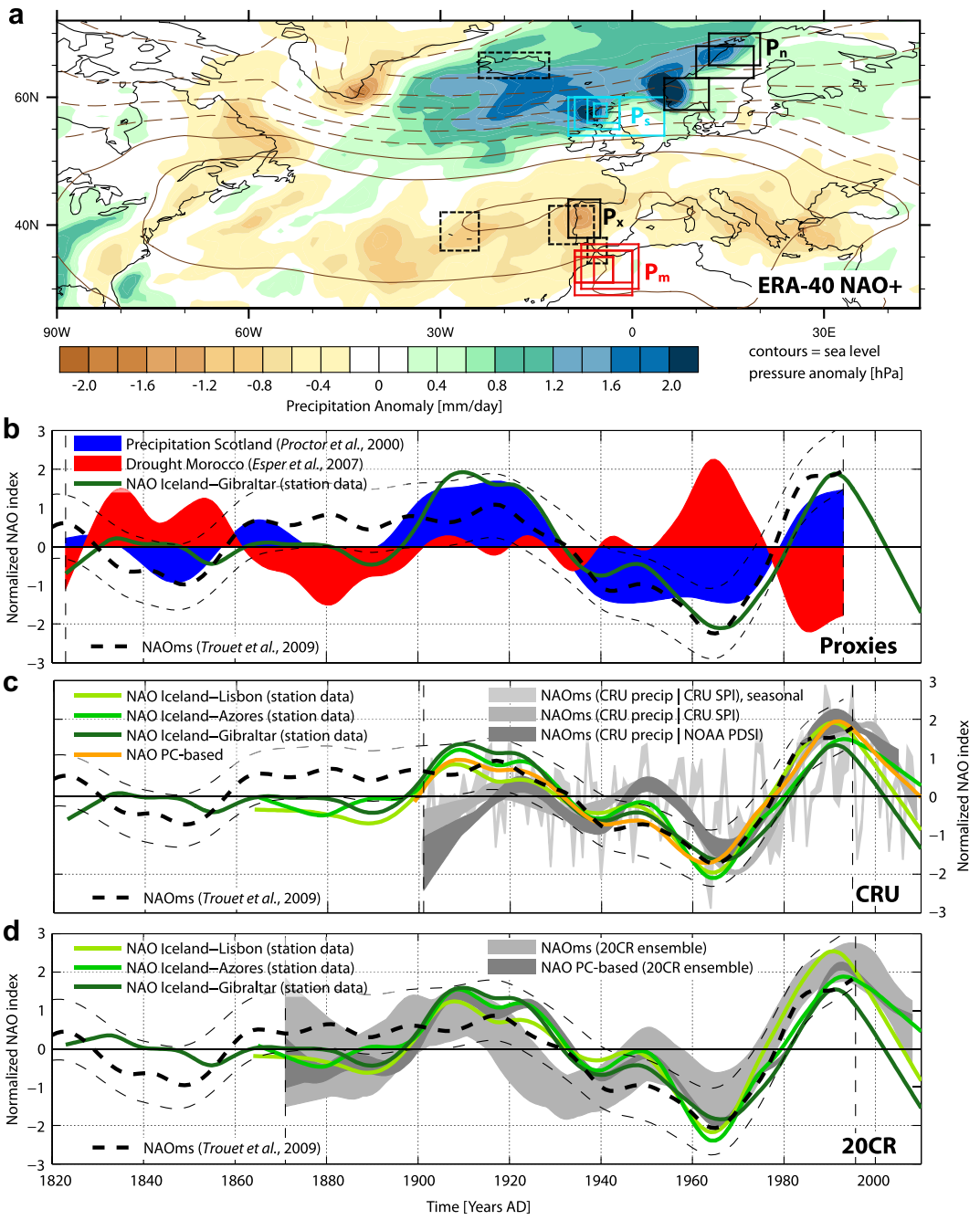

Fig. 2. (a) Precipitation and sea level pressure anomaly composite of the positive NAO phases (December–March PC-based >1.5 – long-term mean) in the 1° × 1° ERA-40 reanalysis (1958–2001 AD; Uppala et al., 2005). Boxes indicate pseudo-proxies regions used in this study: dashed black = sea level pressure, blue = Scotland (P_s), red = Morocco (P_m), solid black = supporting precipitation pseudo-proxies over Scandinavia (P_n) and the Iberian Peninsula (P_x). (b) NAO_{ms} from Trouet et al. (2009) and the proxies on which it is based. (c) NAO_{ms} calculated with CRU (Scotland precipitation vs. Morocco SPI or PDSI). (d) NAO_{ms} and PC-based NAO index calculated from 20CR. (c, d) Along with that up to four instrumental NAO indices are given. The common normalization period is indicated by the vertical dashed lines. (For interpretation of the references to color in this figure legend, the reader is referred to the web version of this article.)

here, as we apply the same method as Trouet et al. (2009) for reasons of optical comparability. Trouet et al. (2009), Fig. 1, is in that respect misleading, as both the individual proxy time series as well as the combined NAO_{ms} are tagged "z-scored", when in fact only the two proxy time series have been normalized. The alternative use of the Palmer Drought Severity Index (PDSI; Dai et al., 2004) in the construction of the NAO_{ms} further illustrates that the choice of the drought index for the Morocco pseudo-proxy has a small effect on the decadal-scale behavior of the NAO_{ms} (Fig. 2c).

When the NAO_{ms} is calculated from 20CR, the results are similar (Fig. 2d). The shift from a negative NAO phase during the 1960s–1970s to a more positive NAO phase during the 1980s–1990s is recorded by the NAO_{ms}. However, when going further back in time the classical indices and the NAO_{ms} start to diverge, despite the considerable range of the 20CR ensemble (4 × 4 different boxes × 56 ensemble members = 896 realizations of NAO_{ms}). At the same time the range of the PC-based (56 realizations) is narrower and follows the station data-based classical NAO indices more closely. This underlines the consistency of the classical NAO indices, which appears to be independent of the data source used (reanalysis or station data). Prior to about 1890 AD, the uncertainty of 20CR precipitation seems to be too large to constrain a clear NAO_{ms} (Fig. 2d).

3.3. Models

3.3.1. Persistence of anomalous NAO phases

Due to the chaotic nature of the atmospheric circulation the coupled models are not expected to reproduce the decadal variability of the actual NAO. On longer time scales (or in case of a strong volcanic eruption), however, external forcing might impact climate variables that are crucial for the NAO. This then provides the opportunity to compare proxy and model NAO indices with regard to their low-frequency trends, i.e., a persistent positive NAO during the MCA and the suggested shift to a more negative NAO from the MCA to the LIA. However, none of the model simulations examined here shows century-scale persistent phases of positive or negative NAO, regardless of the index in question. In the smoothed and normalized time series the models show a few anomalous phases of up to 40–60 years length (Fig. 4). In Fig. 4a the Medieval part of the NAO_{ms} by Trouet et al. (2009) is plotted for comparison. It becomes apparent that the amplitude of the Medieval NAO_{ms} by Trouet et al. (2009) is extraordinary.

As a consequence of not simulating a century-scale persistent positive NAO, the models also do not reproduce the clear shift of the NAO index from positive to more negative values when going from the MCA into the LIA. None of the millennial simulations produces a significant shift (5% level using seasonal values) of the classical NAO indices from the MCA (1000–1250 AD) to the LIA (1450–1700 AD). Still, it is noteworthy that they simulate a reduction of the indices (the largest is −0.18 with unsmoothed and −0.75 with smoothed values). Our ensemble of the medium-resolution CCSM3, that covers the transition phase from the MCA to the LIA (1149–1499 AD), also does not produce significant reductions of the NAO index. Two of the six ensemble members even show an insignificant increase.

3.3.2. Robustness of NAO_{ms}

Regarding the correlation of NAO indices among each other (over the respective length of a simulation), the results are fairly similar to the reanalysis data sets: the correlation among the classical indices is significantly higher than that of the classical indices with the pseudo-proxy NAO_{ms} (Fig. 3a and b). Note, that the correlations in Fig. 3 are done on unsmoothed December–March means. Further, in the remaining part of the paper we show comparisons with PC-based and Iceland-Azores only, as Iceland-Lisbon and Iceland-Gibraltar are very similar to Iceland-Azores ($r = 0.88$–0.93 in 20CR and $r = 0.93$–0.98 in models, both $p < 0.001$). To test whether a correlation between two indices is stable over time, we calculate a 50-year moving window correlation of the two indices over the full length of a millennial simulation. A probability density function (PDF) is then calculated on the resulting time series, providing a measure on of how stable the relationship between two indices is. The PDF of the correlation among the classical indices is narrower than the PDF of the correlation of NAO_{ms} with classical indices (Fig. 3e). This model-independent finding underlines the robustness of the classical indices compared to the NAO_{ms}. The strength of the link between the NAO_{ms} and the classical indices, on the other hand, strongly varies from model to model. CNRM, for example, shows no, or only weak, correlations (−0.01 to +0.36) of NAO_{ms} with the classical NAO indices, while the three ensemble members of MPI all show correlations between 0.38 and 0.61. Also, the sensitivity of the NAO_{ms} to the location of the pseudo-proxy box seems to be model-dependent, as can be seen by the size of the spreads for the different models (Fig. 3e).

In Fig. 4, we select six periods in which disagreement between the NAO_{ms} and the classical indices occurs. In order to better understand the underlying circulation and precipitation pattern, we present a composite analysis over these selected periods on the basis of December–March means (Fig. 5). SLP and precipitation anomalies serve as a reference for the actual climate field simulated during these periods. Regressing the NAO_{ms} onto SLP resembles the circulation pattern indirectly proposed by the pseudo-proxy index. For the latter, the regression coefficients are multiplied by the mean of the unsmoothed NAO_{ms} during the selected period. In the following we classify these six periods into three types by looking at the classical NAO indices in Fig. 4: (i) when they are positive (periods 1 (1251–1265 AD) and 4 (1016–1037 AD); marked in Fig. 4), (ii) neutral, i.e., average within ±0.2, (periods 5 (1212–1237 AD) and 6 (1780–1797 AD)), or (iii) negative (periods 2 (1966–1983 AD) and 3 (1775–1803 AD)).

The cases of positive NAO both feature a clear NAO-positive SLP pattern, however, the locations of the centers of action vary. Especially the southern high pressure center can shift from the Azores (period 1) to the Iberian Peninsula (period 4). The northern center is located in the Iceland-Greenland region. While these situations resemble a positive NAO in the classical sense, they do not necessarily result in the precipitation pattern expected from reanalysis (e.g., Fig. 2a). During period 1 the slight eastward displacement of the high pressure center leads to a dry anomaly over Scotland and wetter conditions over large parts of the Mediterranean, in turn resulting in a negative NAO_{ms}. During period 4 the high pressure center spans from the Azores to Central Europe, resulting to a large extent in the precipitation signal known from reanalysis. However, Scotland lies just in between the wet and dry anomaly, and so the pseudo-proxies produce a neutral NAO_{ms}.

The cases of a neutral NAO both show a ridge of low pressure across the Atlantic which is bordered by elevated pressure in the North and South. In both cases, Scotland and Morocco receive opposite precipitation signals, however, in one case it is Scotland dry-Morocco wet (period 5) while in the other it is vice versa (period 6). Consequently, the NAO_{ms} falsely indicates negative and positive states of the NAO, respectively.

Finally, the cases of negative NAO both feature a negative SLP anomaly in the south with a northern counterpart of elevated pressure. In period 2, the southern low pressure center is weak and the negative NAO arises mainly from the widespread high pressure in the North. Both Scotland and Morocco do not experience a clear precipitation anomaly, which is why the NAO_{ms} is close to zero instead of negative. A similar situation occurs during period 3 when the low pressure center leads to a clear precipitation signal over large parts of the Iberian Peninsula, i.e., just North of Morocco. Morocco itself does not experience this anomaly. As Scotland experiences a weak wet phase, NAO_{ms} wrongly attributes this situation to an NAO-positive phase.

3.3.3. Stabilization of NAO_{ms}

In the previous section situations of disagreement between NAO_{ms} and the classical indices were examined. Reconciling those situations, it becomes apparent how additional pseudo-proxies could help making the NAO_{ms} more robust. For example, from reanalysis we expect Scotland and the Norwegian coast, as well as Morocco and the Iberian Peninsula, to have similar precipitation signals during positive or negative NAO phases (Fig. 2a). However, in several of the previously discussed situations this is not the case: the precipitation anomaly due to a certain NAO phase is displaced slightly to the North, leaving the Morocco or Scotland location without the expected signal. In these situations, the Iberian Peninsula and the Norwegian coast are perfectly situated to captured this signal and valuable information could be gained from proxies in these regions. The chance that a precipitation signal is missed by both Morocco and the Iberian Peninsula (Scotland and the Norwegian coast, respectively) is comparably small.

To test this concept, we define three artificial precipitation proxies along the Norwegian coast (P_n) and one over Portugal/Spain (P_x), marked in Fig. 2a. We average December–March precipitation over a certain geographical box and normalize the time series. The

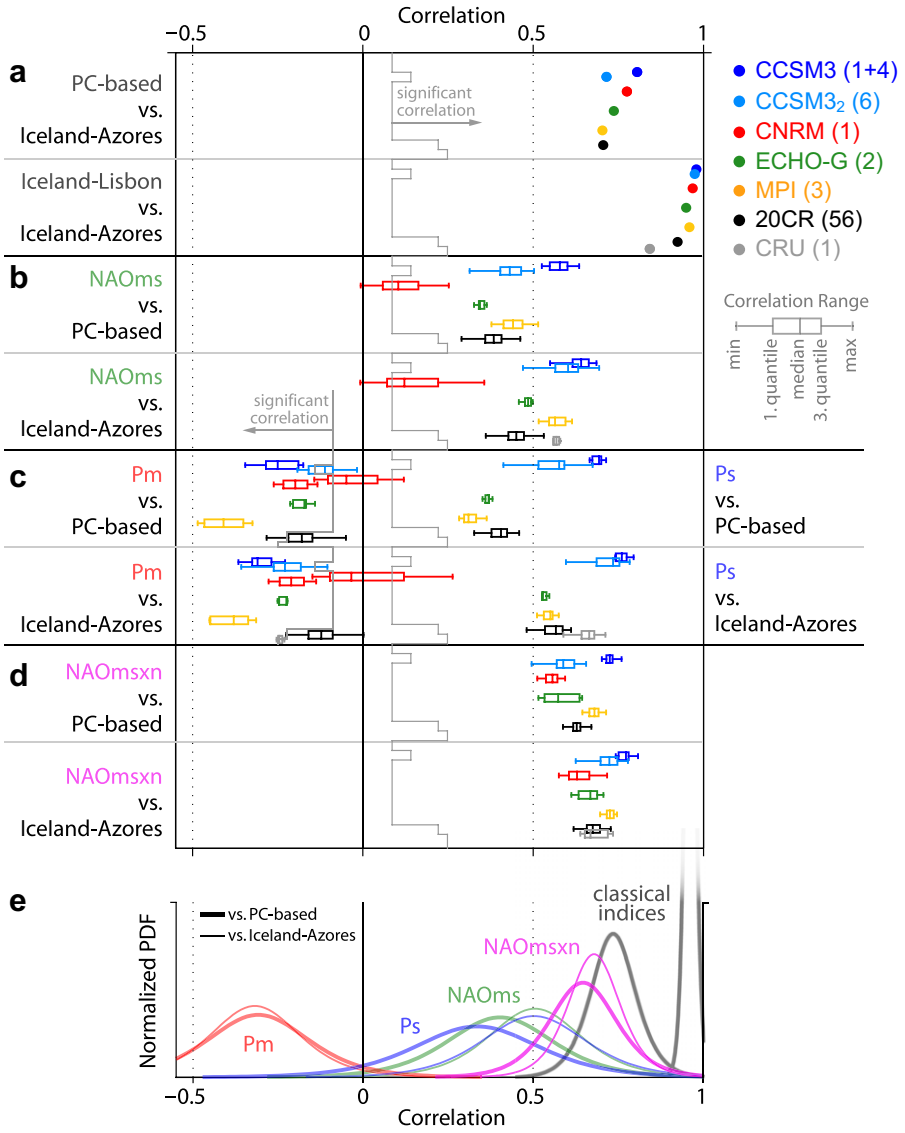

Fig. 3. Correlation of different NAO indices (December–March means, unsmoothed) from models and reanalyses: (a) between Iceland-Azores and two classical NAO indices (PC-based, Iceland-Lisbon), (b) between the perfect pseudo-proxy NAO_{ms} and two classical NAO indices, (c) between Scotland and Morocco precipitation (P_s, P_m) and two classical NAO indices, (d) between the improved NAO_{msxn} and two classical NAO indices. The range of each correlation in (b), (c), and (d) arises from varying the geographical boxes used for the calculation of NAO_{ms}, P_s, P_m, or NAO_{msxn}, as well as from the ensemble (in (a) only the ensemble mean is given). $CCSM3_2$ refers to the ensemble simulations over the MCA-LIA transition phase (1149–1499 AD). The number of ensemble members of a specific model is given in brackets in the upper right corner. The coefficient beyond which a correlation is significant (1% level) is indicated by the vertical gray line. (e) The probability density functions (PDF) are calculated from 50-year moving window correlations between different NAO indices for all the millennial model simulations ($CCSM3_2$ and reanalysis are excluded). Thereby they show the variability of the correlations through the course of a millennium simulation (details see text).

three P_n are then combined with the four P_s to form twelve versions of a new northern regional pseudo-proxy. For the southern center we combine P_x with all four P_m to form four versions of a southern regional pseudo-proxy. In order to determine the weights for such a combination we do a linear regression on the PC-based NAO index from the ensemble mean 20CR data with every combination of P_s and P_n (also taken from 20CR):

$$NAO_{20CR} = \beta_{sij} \cdot P_{si} + \beta_{nij} \cdot P_{nj} + \epsilon_{ij}, \quad (1)$$

where i and j indicate the different geographical boxes used, β_{sij} and β_{nij} are the regression coefficients associated with a certain combination of P_{si} and P_{nj}, and ϵ_{ij} is the residual to be minimized. Solving the model for all combinations of geographical boxes results in twelve pairs of the regression coefficients (the same is done for P_{mi} and P_x, resulting in four pairs of coefficients). All coefficients of a specific P are averaged, leaving one coefficient for each P ($\overline{\beta_{sij}}$, $\overline{\beta_{nij}}$, $\overline{\beta_{mi}}$, $\overline{\beta_{xi}}$). This way we neglect differences within one region (e.g., among the three Scandinavia pseudo-proxies) and imply that it does not matter which pseudo-proxy from that region is used. Thereby, we also introduce some uncertainty compared to the prefect approach of calculating coefficients individually for each box and each model. Each pair of coefficients ($\overline{\beta_{sij}}/\overline{\beta_{nij}}$, $\overline{\beta_{mi}}/\overline{\beta_{xi}}$) is then scaled so that the sum of the two is one, representing the weights of P_s relative to P_n (P_m relative to P_x, respectively). According to this procedure, the weights are calculated and applied as follows to create a new NAO index

$$NAO_{msxn} = (0.52 \cdot P_s + 0.48 \cdot P_n) - (0.19 \cdot P_m + 0.81 \cdot P_x). \quad (2)$$

NAO_{msxn} is calculated for all models and reanalysis data sets with the weights from Eq. (2) and tested in the same manner as

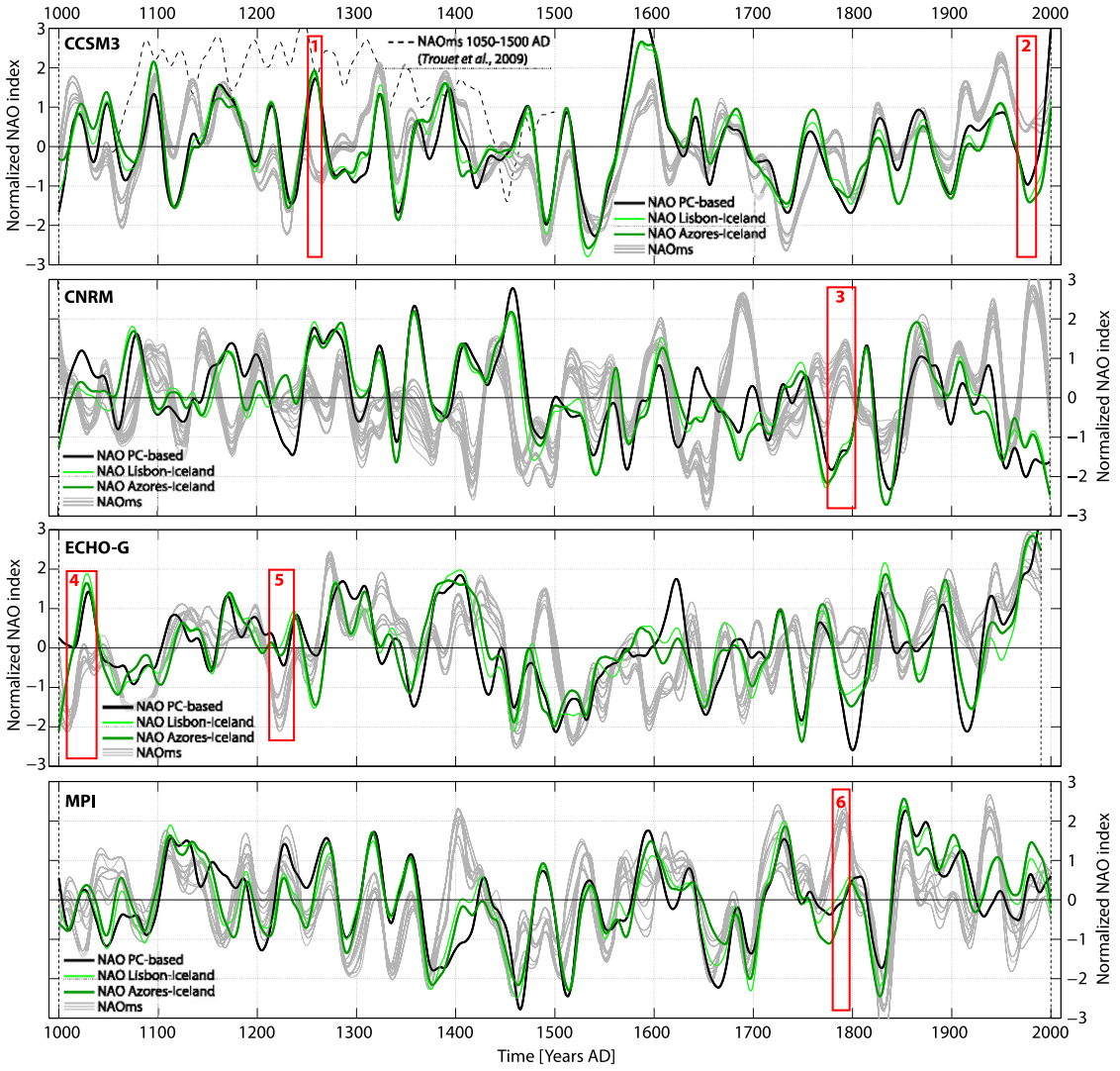

Fig. 4. NAO indices from four different models (denoted in the upper left corner of each subplot). Shown are the classical NAO indices PC-based, Lisbon-Iceland, and Azores-Iceland together with the NAO_{ms}, all calculated from model output. The time series are normalized over the common period indicated by the vertical dashed lines. A part of the NAO_{ms} from Trouet et al. (2009) is given in (a) for comparative reasons. For the models with an ensemble, one representative simulation was chosen. Exemplary periods of disagreement between the classical NAO indices and the NAO_{ms} are framed red and referred to in Fig. 5.

NAO_{ms}. The new NAO_{msxn} on average correlates better with classical indices than does the NAO_{ms}: the correlation over the full length of the reanalyses or the model simulations is always larger than 0.49 (Fig. 3d). Thus this convergence of the different models in terms of full-length correlation illustrates that NAO_{msxn} is a robust index, independent of the models' individual representation of precipitation. For example, while NAO_{ms} appeared not to work in CNRM (correlations close to zero), NAO_{msxn} shows comparable skill for all models. This increased robustness of the new index is also reflected in the PDFs of the moving window correlation. They are narrower, indicating that there are fewer 50-year periods of disagreement in the millennial simulations (Fig. 3e). Also, the number of winters in which the NAO_{msxn} still disagrees with the classical indices (i.e., indices differing by more than 1) is reduced by about 50% compared to NAO_{ms} across all models (not shown). All analyses presented in this section are also applied to the multi-century control simulations of the transient simulations, excluding the CNRM for which no control simulation was available (not shown). In all cases, the results were found to be the same, i.e., the correlations do not significantly differ from the transient simulations and no century-long persistent anomalous NAO phases were found. It therefore appears that the results are not dependent on the transient external forcing.

4. Discussion

From reanalyses and instrumental records it becomes apparent that the NAO_{ms} fails to verify against classical NAO indices during the early 20th and 19th century, as both proxies used in NAO_{ms} are reversed in their relation to the NAO during that time. While the individual proxies used in Trouet et al. (2009) represent well verified reconstructions (see Proctor et al., 2000; Esper et al., 2007), their relation to the NAO is more difficult to proof. The challenges inherent in the use of other climate variables than sea level pressure to describe the NAO are illustrated also by the comparison of NAO_{ms} with other existing NAO reconstructions (Table S1, supporting online material for Trouet et al., 2009): there exist correlations among these reconstructions, however, they temporally vary and they are not always significant. It seems therefore more likely that the proxies in NAO_{ms} are not fully representative of the NAO during the 19th century.

When calculated from model output, the concept of NAO_{ms} reveals similar weaknesses. The correlation with classical indices is

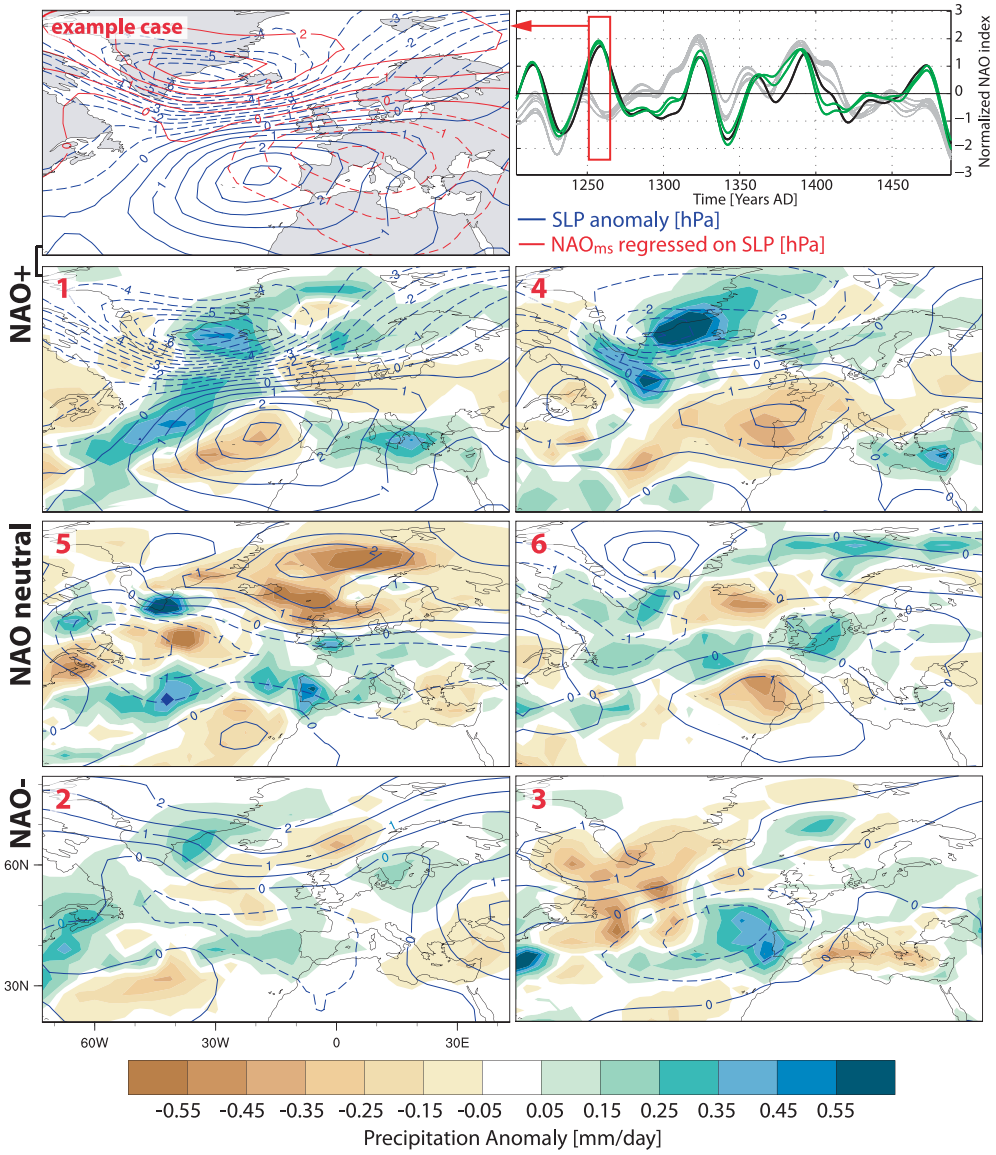

Fig. 5. Periods of disagreement between the classical NAO indices and the NAO_{ms} in the models. The first row illustrates example case #1, the legend for the right panel is the same as in Fig. 4. In the example case #1 the red contours are the regression of the mean NAO_{ms} onto the December–March SLP during the specific period. The second, third, and fourth row show examples for positive, neutral, and negative phases of NAO, respectively. The red numbers correspond to the frames in Fig. 4. Shown are the December–March precipitation (shading) and sea level pressure (SLP; blue contours) anomalies from the long-term mean. (For interpretation of the references to color in this figure legend, the reader is referred to the web version of this article.)

significantly lower than when classical indices are correlated among themselves. To a certain degree this comes as no surprise, as the classical indices are based directly on sea level pressure while the NAO_{ms} uses precipitation, for which the NAO provides a smaller amount of explained variance (e.g., Dai et al., 1997). However, in the model simulations, the correlation between NAO_{ms} and classical indices is also not stable over time, i.e., over the last millennium. This again points to the possibility that the NAO_{ms} at times does not necessarily represent the NAO in the classical sense. Further, this finding is coherent with other model studies that found the relationship between NAO and precipitation not to be stable (Vicente-Serrano and Lopez-Moreno, 2008). In other words, the locations of the proxies in NAO_{ms} are likely not optimal or sufficient to capture the signal from the large-scale circulation pattern. In particular, the Morocco proxy does not add significantly to the robustness of the NAO_{ms} as it often lies just beyond the border of the southern hydrological center of action during anomalous NAO phases. To some extent this is true also for the Scotland proxy where the precipitation band associated with the NAO can be located just north of the site. Additionally, bearing in mind the documented (Jung and Hilmer, 2001) and modeled (Ulbrich and Christoph, 1999; Raible et al., 2006) possibility of shifting NAO centers of action, the use of few and not particularly well located proxies casts doubt on the credibility of a reconstruction based on them.

Therefore, by complementing the Scotland proxy with a precipitation proxy from along the Norwegian coast, the description of the northern center of action of the NAO becomes substantially more robust. The same holds true for the southern center of action when we support Morocco by a precipitation proxy from the Iberian Peninsula. The so created new NAO index has a significant correlation with classical NAO indices of at least 0.49 for all models, reanalyses, and combinations of geographical boxes. Also, the temporal stability of the so created index is higher than of the NAO_{ms}, as the situations of disagreement with classical indices are greatly reduced in number. This qualifies the new index to be a robust description of the actual NAO behavior. Note, however, that in reality proxies to

complement the NAO_{ms} by Trouet et al. (2009) at these locations have yet to be discovered. Additionally, in our minimalistic approach we do not consider potential other proxies (e.g., temperature) at other locations that might further improve the reconstruction (as done in, e.g., Luterbacher et al. (2002); Cook et al. (2002)).

Regarding the occurrence of persistent anomalous phases of the NAO, models do not simulate such phases with only the realistic natural and anthropogenic forcing applied (see also Yiou et al., 2012). This finding is valid for all the NAO indices, also the NAO_{ms}. At the same time the models produce a realistic temperature evolution over the study area, indicating that an NAO phase change of the amplitude suggested by Trouet et al. (2009) is not a prerequisite for the explanation of the MCA-LIA climate transition. Here, new experimental setups with artificially imposed persistent NAO phases are needed (similar to, e.g., Palastanga et al., 2011). Thereby, insights might also be gained concerning the question whether models generally lack the capability of simulating persistent phases of the NAO or if the loss of variance in the Medieval part of the NAO_{ms} (which largely originates from the Scotland proxy) is an artifact of processes not related to the atmospheric circulation. By using several models with different resolutions we provide a large sample of physically consistent analogs to reality. Thereby, we can reduce, but not exclude, the chance that a severe model bias undermines the credibility of the results. In our study, eleven out of thirteen model simulations on average produce a reduction of the classical NAO indices from the MCA to the LIA. Even though none of these are significant, a small shift from a more positive to a more negative NAO phase cannot be excluded.

The pseudo-proxy exercise further shows that a smoothed and normalized NAO time series at times can have a larger mean than the annual values it is based on. This complicates the interpretation of the +2 amplitude of the NAO_{ms} during the MCA and calls for a new assessment on what the actual multi-decadal variability of atmospheric circulation in the North Atlantic-European region has been in the first half of the past millennium.

Note, that the pseudo-proxy exercise is in many respects an idealized and simplified experiment as in reality a precipitation proxy inherits noise and measurement errors that are absent in our study. Even two NAO reconstructions using multiple and well distributed proxies do not necessarily agree, as can be shown at the example of Cook et al. (2002) vs. Luterbacher et al. (2002), and for longer time scales in Raible et al. (2005). We can nevertheless conclude that precipitation proxies in adequate locations are suited to reconstruct past circulation regimes, as suggested by Zorita and González-Rouco (2002). However, a reconstructed index' proposed physical meaning has to withstand thorough tests based on model simulations and reanalyses such as presented here.

5. Conclusions

The robustness of the proxy-based NAO reconstruction (NAO_{ms}) by Trouet et al. (2009) is tested in a perfect pseudo-proxy approach using comprehensive climate models, reanalysis data sets, and instrumental records. The failure of NAO_{ms} to verify against classical NAO indices during the early 20th and 19th century urges future reconstructions to extend the calibration/validation period beyond the 20th century using reanalyses and instrumental data – a conclusion that was already reached a decade ago.

Model simulations reveal that the proxy locations used in the reconstruction by Trouet et al. (2009) are not always able to capture the NAO precipitation signal, resulting in decade-long periods of disagreement of NAO_{ms} with the classical NAO indices. By using additional pseudo-proxies in the vicinity of the existing proxies we are able to catch the non-stationary NAO centers of action and improve the stability of the reconstruction concept. Thereby, we also provide a physical explanation for the weaknesses of the NAO_{ms} concept and lay out a framework of tests for future reconstructions.

Further, results from transient model simulations neither support a persistent positive NAO during the MCA, nor a strong phase shift of the NAO when passing into the LIA. The here presented evidence should motivate both the proxy and model community to work toward a revised assessment of the role of the NAO during the first half of the last millennium.

Acknowledgments

We gratefully acknowledge Fidel González-Rouco, Didier Swingedouw, Johann Jungclaus, and Dominik Hofer for providing the simulations, Laura Fernández-Donado and Niklaus Merz for valuable discussion, and two anonymous reviewers for constructive comments. We are grateful to the ECMWF in Reading, UK (ERA-40), the NOAA/OAR/ESRL PSD in Boulder, USA (20CR), the CRU in Norwich, UK (CRU reanalysis), and the CAS at NCAR in Boulder, USA (NAO indices) for providing access to data and to the NCAR for providing the code of the CCSM3 model. This study is supported by the National Centre of Competence in Research (NCCR) Climate funded by the Swiss National Science Foundation, and the European Commission Past4Future project (Grant Number: 243908. 2010–2014). The simulations for this study were performed on a CRAY XT5 at the Swiss National Supercomputing Centre (CSCS) in Manno.

References

Appenzeller, C., Stocker, T., Anklin, M., 1998. North Atlantic Oscillation dynamics recorded in Greenland ice cores. Science 282, 446–449.
Casty, C., Raible, C.C., Stocker, T.F., Wanner, H., Luterbacher, J., 2007. A European pattern climatology 1766–2000. Climate Dynamics 29, 791–805.
Compo, G.P., Whitaker, J.S., Sardeshmukh, P.D., Matsui, N., Allan, R.J., Yin, X., Gleason Jr., B.E., Vose, R.S., Rutledge, G., Bessemoulin, P., Broennimann, S., Brunet, M., Crouthamel, R.I., Grant, A.N., Groisman, P.Y., Jones, P.D., Kruk, M.C., Kruger, A.C., Marshall, G.J., Maugeri, M., Mok, H.Y., Nordli, O., Ross, T.F., Trigo, R.M., Wang, X.L., Woodruff, S.D., Worley, S.J., 2011. The twentieth century reanalysis project. Quarterly Journal of the Royal Meteorological Society 137, 1–28.
Cook, E., D'Arrigo, R., Briffa, K., 1998. A reconstruction of the North Atlantic Oscillation using tree-ring chronologies from North America and Europe. The Holocene 8, 9–17.
Cook, E.R., D'Arrigo, R.D., Mann, M.E., 2002. A well-verified, multiproxy reconstruction of the winter North Atlantic Oscillation index since A.D. 1400. Journal of Climate 15, 1754–1764.
Cullen, H., D'Arrigo, R., Cook, E., Mann, M., 2001. Multiproxy reconstructions of the North Atlantic Oscillation. Paleoceanography 16, 27–39.
Dai, A., Fung, I., DelGenio, A., 1997. Surface observed global land precipitation variations during 1900–88. Journal of Climate 10, 2943–2962.
Dai, A., Trenberth, K., Qian, T., 2004. A global dataset of Palmer Drought Severity Index for 1870–2002: relationship with soil moisture and effects of surface warming. Journal of Hydrometeorology 5, 1117–1130.
Esper, J., Frank, D., Buentgen, U., Verstege, A., Luterbacher, J., 2007. Long-term drought severity variations in Morocco. Geophysical Research Letters 34.
Glueck, M.F., Stockton, C.W., 2001. Reconstruction of the North Atlantic Oscillation, 14291983. International Journal of Climatology 21, 1453–1465.
González-Rouco, J., Beltrami, H., Zorita, E., von Storch, H., 2006. Simulation and inversion of borehole temperature profiles in surrogate climates: spatial distribution and surface coupling. Geophysical Research Letters 33.
Gray, L.J., Beer, J., Geller, M., Haigh, J.D., Lockwood, M., Matthes, K., Cubasch, U., Fleitmann, D., Harrison, G., Hood, L., Luterbacher, J., Meehl, G.A., Shindell, D., van Geel, B., White, W., 2010. Solar influences on climate. Reviews of Geophysics 48.
Guttman, N., 1999. Accepting the standardized precipitation index: a calculation algorithm. Journal of the American Water Resources Association 35, 311–322.
Hofer, D., Raible, C.C., Stocker, T.F., 2011. Variations of the Atlantic meridional overturning circulation in control and transient simulations of the last millennium. Climate of the Past 7, 133–150.
Hurrell, J.W., 1995. Decadal trends in the North Atlantic Oscillation: regional temperatures and precipitation. Science 269, 676–679.
IPCC, 2001. Climate Change 2001, the Scientific Basis. Intergovernmental Panel on Climate Change. Cambridge University Press.
Jones, P.D., Jonsson, T., Wheeler, D., 1997. Extension to the North Atlantic Oscillation using early instrumental pressure observations from Gibraltar and south-west Iceland. International Journal of Climatology 17, 1433–1450.
Jung, T., Hilmer, M., 2001. The link between the North Atlantic Oscillation and Arctic Sea ice export through Fram Strait. Journal of Climate 14, 3932–3943.

Jungclaus, J.H., Lorenz, S.J., Timmreck, C., Reick, C.H., Brovkin, V., Six, K., Segschneider, J., Giorgetta, M.A., Crowley, T.J., Pongratz, J., Krivova, N.A., Vieira, L.E., Solanki, S.K., Klocke, D., Botzet, M., Esch, M., Gayler, V., Haak, H., Raddatz, T.J., Roeckner, E., Schnur, R., Widmann, H., Claussen, M., Stevens, B., Marotzke, J., 2010. Climate and carbon-cycle variability over the last millennium. Climate of the Past 6, 723–737.

Kuettel, M., Xoplaki, E., Gallego, D., Luterbacher, J., Garcia-Herrera, R., Allan, R., Barriendos, M., Jones, P.D., Wheeler, D., Wanner, H., 2010. The importance of ship log data: reconstructing North Atlantic, European and Mediterranean sea level pressure fields back to 1750. Climate Dynamics 34, 1115–1128.

Kutzbach, J., 1970. Large-scale features of monthly mean Northern Hemisphere anomaly maps of sea-level pressure. Monthly Weather Review 98, 708–716.

Lehner, F., Raible, C.C., Stocker, T.F., Hofer, D., in press in press. The freshwater balance of polar regions in transient simulations from 1500 to 2100 AD using a comprehensive coupled climate model. Climate Dynamics.

Luterbacher, J., Schmutz, C., Gyalistras, D., Xoplaki, E., Wanner, H., 1999. Reconstruction of monthly NAO and EU indices back to AD 1675. Geophysical Research Letters 26, 2745–2748.

Luterbacher, J., Xoplaki, E., Dietrich, D., Jones, P.D., Davies, T.D., Portis, D., Gonzalez-Rouco, J.F., von Storch, H., Gyalistras, D., Casty, C., Wanner, H., 2002. Extending North Atlantic Oscillation reconstructions back to 1500. Atmospheric Science Letters 2, 114–124.

Mangini, A., Spotl, C., Verdes, P., 2005. Reconstruction of temperature in the Central Alps during the past 2000 yr from a delta(18)O stalagmite record. Earth and Planetary Science Letters 235, 741–751.

Mann, E.M., Zhang, Z., Rutherford, S., Bradley, R.S., Hughes, M.K., Shindell, D., Ammann, C., Faluvegi, G., Ni, F., 2009. Global signatures and dynamical origins of the Little Ice Age and Medieval Climate Anomaly. Science 326, 1256–1260.

Mann, M., 2002. Large-scale climate variability and connections with the Middle East in past centuries. Climatic Change 55, 287–314.

Meeker, L., Mayewski, P., 2002. A 1400-year high-resolution record of atmospheric circulation over the North Atlantic and Asia. The Holocene 12, 257–266.

Mitchell, T.D., Jones, P.D., 2005. An improved method of constructing a database of monthly climate observations and associated high-resolution grids. International Journal of Climatology 25, 693.

Palastanga, V., van der Schrier, G., Weber, S.L., Kleinen, T., Briffa, K.R., Osborn, T.J., 2011. Atmosphere and ocean dynamics: contributors to the European Little Ice Age? Climate Dynamics 36, 973–987.

Pinto, J.G., Raible, C.C., 2012. Past and recent changes in the North Atlantic Oscillation. Wiley Interdisciplinary Reviews: Climate Change 3, 79–90.

Portis, D., Walsh, J., El Hamly, M., Lamb, P., 2001. Seasonality of the North Atlantic Oscillation. Journal of Climate 14, 2069–2078.

Proctor, C., Baker, A., Barnes, W., Gilmour, R., 2000. A thousand year speleothem proxy record of North Atlantic climate from Scotland. Climate Dynamics 16, 815–820.

Raible, C.C., Casty, C., Luterbacher, J., Pauling, A., Esper, J., Frank, D.C., Buentgen, U., Roesch, A.C., Tschuck, P., Wild, M., Vidale, P.-L., Schaer, C., Wanner, H., 2006. Climate variability-observations, reconstructions, and model simulations for the Atlantic-European and Alpine region from 1500–2100 AD. Climatic Change 79, 9–29.

Raible, C.C., Stocker, T.F., Yoshimori, M., Renold, M., Beyerle, U., Casty, C., Luterbacher, J., 2005. Northern hemispheric trends of pressure indices and atmospheric circulation patterns in observations, reconstructions, and coupled GCM simulations. Journal of Climate 18, 3968–3982.

Rodrigo, F., Pozo-Vazquez, D., Esteban-Parra, M., Castro-Diez, Y., 2001. A reconstruction of the winter North Atlantic Oscillation index back to AD 1501 using, documentary data in southern Spain. Journal of Geophysical Research 106, 14805–14818.

Rogers, J., 1984. The association between the North-Atlantic Oscillation and the Southern Oscillation in the Northern Hemisphere. Monthly Weather Review 112, 1999–2015.

Salas-Mélia, D., Chauvin, F., Déqué, M., Douville, H., Guérémy, J.F., Marquet, P., Planton, S., Royer, J.F., Tyteca, S., 2005. Description and Validation of the CNRM-CM3 Global Coupled Model. Tech. rep. CNRM/GMGEC.

Schmutz, C., Luterbacher, J., Gyalistras, D., Xoplaki, E., Wanner, H., 2000. Can we trust proxy-based NAO index reconstructions? Geophysical Research Letters 27, 1135–1138.

Shapiro, A.I., Schmutz, W., Rozanov, E., Schoell, M., Haberreiter, M., Shapiro, A.V., Nyeki, S., 2011. A new approach to the long-term reconstruction of the solar irradiance leads to large historical solar forcing. Astronomy and Astrophysics 529.

Steinhilber, F., Beer, J., Froehlich, C., 2009. Total solar irradiance during the Holocene. Geophysical Research Letters 36.

Stoner, A.M.K., Hayhoe, K., Wuebbles, D.J., 2009. Assessing General Circulation Model simulations of atmospheric teleconnection patterns. Journal of Climate 22, 4348–4372.

Swingedouw, D., Terray, L., Cassou, C., Voldoire, A., Salas-Mélia, D., Servonnat, J., 2011. Natural forcing of climate during the last millennium: fingerprint of solar variability. Climate Dynamics 36, 1349–1364.

Trouet, V., Esper, J., Graham, N.E., Baker, A., Scourse, J.D., Frank, D.C., 2009. Persistent positive North Atlantic Oscillation mode dominated the Medieval Climate Anomaly. Science 324, 78–80.

Trouet, V., Scourse, J.D., Raible, C.C., 2012. North Atlantic storminess and Atlantic Meridional Overturning Circulation during the last Millennium: reconciling contradictory proxy records of NAO variability. Global and Planetary Change 84–85, 48–55.

Ulbrich, U., Christoph, M., 1999. A shift of the NAO and increasing storm track activity over Europe due to anthropogenic greenhouse gas forcing. Climate Dynamics 15, 551–559.

Uppala, S., Kallberg, P., Simmons, A., Andrae, U., Bechtold, V., Fiorino, M., Gibson, J., Haseler, J., Hernandez, A., Kelly, G., Li, X., Onogi, K., Saarinen, S., Sokka, N., Allan, R., Andersson, E., Arpe, K., Balmaseda, M., Beljaars, A., Van De Berg, L., Bidlot, J., Bormann, N., Caires, S., Chevallier, F., Dethof, A., Dragosavac, M., Fisher, M., Fuentes, M., Hagemann, S., Holm, E., Hoskins, B., Isaksen, L., Janssen, P., Jenne, R., McNally, A., Mahfouf, J., Morcrette, J., Rayner, N., Saunders, R., Simon, P., Sterl, A., Trenberth, K., Untch, A., Vasiljevic, D., Viterbo, P., Woollen, J., 2005. The ERA-40 re-analysis. Quarterly Journal of the Royal Meteorological Society 131, 2961–3012.

Vicente-Serrano, S.M., Lopez-Moreno, J.I., 2008. Nonstationary influence of the North Atlantic Oscillation on European precipitation. Journal of Geophysical Research 113.

Vinther, B., Andersen, K., Hansen, A., Schmith, T., Jones, P., 2003. Improving the Gibraltar/Reykjavik NAO index. Geophysical Research Letters 30.

Wanner, H., Brönnimann, S., Casty, C., Gyalistras, D., Luterbacher, J., Schmutz, C., Stephenson, D.B., Xoplaki, E., 2001. North Atlantic Oscillation – concepts and studies. Surveys in Geophysics 22, 321–382.

Yiou, P., Servonnat, J., Yoshimori, M., Swingedouw, D., Khodri, M., Abe-Ouchi, A., 2012. Stability of weather regimes during the last millennium from climate simulations. Geophysical Research Letters.

Zorita, E., González-Rouco, F., 2002. Are temperature-sensitive proxies adequate for North Atlantic Oscillation reconstructions? Geophysical Research Letters 29.

Zorita, E., Gonzalez-Rouco, F., Legutke, S., 2003. Testing the Mann et al. (1998) approach to paleoclimate reconstructions in the context of a 1000-yr control simulation with the ECHO-G coupled climate model. Journal of Climate 16, 1378–1390.